3.2. Stepwise auroral bulge evolution during expansion phase: June 6-7, 1989 event

Abstract.

We have analyzed in detail the auroral bulge evolution during the expansion phase of an isolated substorm, which was observed by the UV imager aboard AKEBONO. It was found that there were three distinct stages in the evolution. The Stage-1 was characterized by the rapid poleward and rapid azimuthal (predominantly westward) expansions in a short time (about 2 min). The next Stage-2 was characterized by the very slow poleward and slower and continuous azimuthal expansions. There was a certain period for transition between the Stage-1 and the Stage-2, and it was characterized by the very slow poleward and rapid eastward expansions. The last Stage-3 started about 11 min after the onset, and was characterized by a sudden re-activation of the rapid poleward and rapid azimuthal expansions. The re-activation started around the initial onset meridian, and then spread both eastward and westward. At the azimuthal front, the expansion first occurred at the lowest latitudes, spread poleward to around the ceiling latitudes of the Stage-1, and then spread further poleward after a brief interval. Hence, the local expansion also had three distinct stages as the global one. The ground-based observations showed that the ceiling latitude of the local first stage was very close to the latitude of a characteristic auroral activity that appeared near the ionospheric PSBL (plasma sheet boundary layer) region a few minutes before the onset. The further poleward expansion during the local third stage started with a significant intensification of the poleward-most auroral activity. During the local third stage, the bright electron auroral region was bifurcated into a poleward expanding part and an equatorward moving part. The proton auroral emission coexisted in the bulge during the local first and second stages, and almost disappeared soon after the bifurcation during the local third stage. Based on these observations, we discussed the evolution in the magnetosphere during the expansion phase.

1. Introduction

In the classical morphology of *Akasofu* [1964], which is based on a great number of ground-based all-sky camera observations, the expansion (originally "expansive") phase of an auroral substorm was divided into three stages. The Stage-1 starts with a sudden brightening of a most equatorward arc a few thousand kilometers in length approximately centered at the midnight meridian. The brightened arc rapidly starts to move poleward. This stage lasts for 0-5 min. In the following Stage-2, which occurs within 5-10 min after the onset, an auroral bulge is formed around the midnight sector, and rapidly expands poleward, westward and eastward. At the western edge of the expanding bulge, a large scale fold called a westward travelling surge (WTS) is formed. In the next Stage-3, which occurs within 10-30 min after the onset, the poleward front of the bulge around the midnight meridian reaches its most

poleward point. The WTS continues to move westward. To the lower latitude of the bulge, isolated and cloud-like patches appear and drift westward and eastward in the evening and morning sectors, respectively. This initial morphology has been modified and refined along the new results obtained with the various ground-based and satellite-based auroral observations, so far.

The global evolution of the bulge has been studied using various satellite auroral imagers. The initial brightening tends to occur preferably in a pre-midnight localized region around 23 hr MLT (magnetic local time) within the auroral oval with its spatial extent of less than 1 hour [e.g. *Frank and Craven*, 1988; *Murphree et al.*, 1991; *Elphinstone et al.*, 1995a; *Liou et al.*, 2001]. After the expansion of the bulge reaches maximum, the high latitude edge of the bulge is intensified and a chain of spirals (vortex street) often appears there, whereas the emission intensity within the bulge becomes weak. As a result, an emission gap appears between the most poleward discrete auroral activity and the most equatorward diffuse auroral oval. Such a configuration is usually called the "double oval" [*Cogger and Elphinstone*, 1992; *Elphinstone et al.*, 1995b]. A large scale WTS is located at the western edge of the bulge, linking those two auroral regions in the "double oval" configuration [*Cogger and Elphinstone*, 1992].

The proton auroral substorm and its relationship with the electron auroral substorm have been studied using the ground-based observations [e.g. *Montbriand*, 1971; *Fukunishi*, 1975b; *Oguti*, 1973; *Takahashi and Fukunishi*, 2001] and the satellite-based global observations [e.g. *Mende et al.*, 2001]. These studies showed that the initial brightening occurs around the poleward edge of the main proton auroral oval, and the proton auroral emission coexists within the poleward expanding bulge especially in the initial stage. As the bulge expands, the bright proton auroral region extends into the duskside from the eastern edge of the bulge, whereas the bright electron auroral region extends into the dawnside from the western edge of the bulge [e.g. *Fukunishi*, 1975b; *Mende et al.*, 2001].

Many previous observations showed that there are several steps in the auroral bulge evolution. The initial expansion is frequently observed to be very rapid. *Shepherd and Murphree* [1991] showed an example where the bulge expanded poleward and reached a ceiling latitude about 1 min after the onset. After that time, the bulge expanded mainly in the azimuthal direction. In the event of *Rostoker et al.* [1987b] (their Fig. 3.2.1), the initial bulge reached a ceiling latitude about 3 min after the onset. After that time, the bulge expanded mainly in the azimuthal direction until a further poleward expansion started later. The events of *Liou et al.* [1999] (their Plates 1 and 3) and *Liou et al.* [2000a] (their Fig. 3.2.1) also showed such a rapid poleward expansion. Judging from their figures, the bulge reached a ceiling latitude within 3-5 min after the onset. *Kaneda and Yamamoto* [1991] pointed out that there should be two distinct stages in the initial bulge evolution; initial brightening and flaring-up. The initial brightening stage lasts 3-5 min with increases in brightness but no appreciable expansion of the activated region, while in the flaring-up stage, the activated

region expands rapidly within a few minutes and grows into the auroral bulge filled up with active forms.

It is also frequently observed that a further expansion of the bulge occurs in later time. One event of *Brittnacher et al.* [1999] (their Plate 1) showed that the further poleward expansion occurred about 12 min after the onset. Three events of *Henderson et al.* [1998] showed that the further expansion occurs with an activation of the most poleward arc system and a creation of an N-S (north-south aligned) auroral structure within the bulge. The event of *Rostoker et al.* [1987b] also showed that a further poleward expansion occurred about 6-9 min after the onset, and it coincided with an intensification of the most poleward region. They showed that such an intensification and a further poleward expansion episodically occurred several times afterward. In the event of *Hones et al.* [1987], the further poleward expansion, which they called the "poleward leap", occurred about 20 min after the onset. Almost all the observations mentioned above showed that the "double oval" configuration clearly appeared only after the further poleward expansion occurred.

Although such a stepwise evolution of the auroral bulge seems to be a common feature during the expansion phase of a substorm, to our knowledge, there are few previous works that showed the full process of the stepwise evolution and pointed out its importance in the context of the magnetospheric substorm. In this study, we have analyzed in detail one substorm event where such kind of the stepwise evolution was observed. This substorm was the first one which occurred after a southward turning of the interplanetary magnetic field (IMF), and had a well-defined growth phase of about 1 hour duration. The details of the growth phase phenomena of this substorm were described in our preceding paper (paper-1). The southward IMF condition continued through the growth phase to the expansion phase of the substorm. A magnetic storm started with a sudden commencement (SC) which occurred before the southward turning of the IMF, and developed into a "moderate storm [cf. *Gonzalez et al., 1994*]" (minimum Dst = -86 nT). The expansion phase of this substorm occurred during the main phase of the storm. In that sense, this substorm was a "storm-time substorm". In the magnetosphere, a significant injection of energetic particles was observed at the geosynchronous orbit during the expansion phase.

We show the observational results in section 2. We discuss the results in section 3, and summarize this study in section 4.

2. Observations

2.1. Solar wind and geomagnetic conditions

The expansion phase onset of an isolated substorm occurred at 00:41:40 UT on June 7, 1989, which is determined by the Pi2 activity at Hermanus (HER) station and the global auroral activity observed by the UV auroral TV camera (ATV-UV) aboard the AKEBONO satellite. On the previous day, a geomagnetic sudden commencement (SC) occurred at 23:14

UT, and the interplanetary magnetic field (IMF) turned southward at 23:40 UT after a preceding long northward period. The expansion phase of this substorm progressed under a high solar wind pressure (both dynamic and static) and a steady southward IMF conditions. The southward IMF condition continued until 02:27 UT on June 7. The recovery phase started after that time. The geomagnetic condition before the SC was very quiet, and a significant evolution of the growth phase was observed after the southward turning of the IMF. After the SC, a magnetic storm developed and reached its maximum depression of -86 nT in Dst at 12 UT on June 7. Details of the IMF and the solar wind data and the growth phase evolution were described in the paper-1. In this study, we concentrate on the detailed evolution during the expansion phase.

2.2. Instrumentation

The evolution of the global auroral activity in this substorm was observed by the ATV-UV over the Antarctic region from 00:37:28 UT until 01:05:00 UT on June 7. Specifications of the ATV-UV are described in detail by *Oguti et al.* [1990]. ATV-UV can take snapshot images in the wave length range of 115.0-139.0 nm with the highest time resolution of the satellite spin period, about 8 sec. During this event, time intervals in one observation sequence were 8-8-8-40 sec.

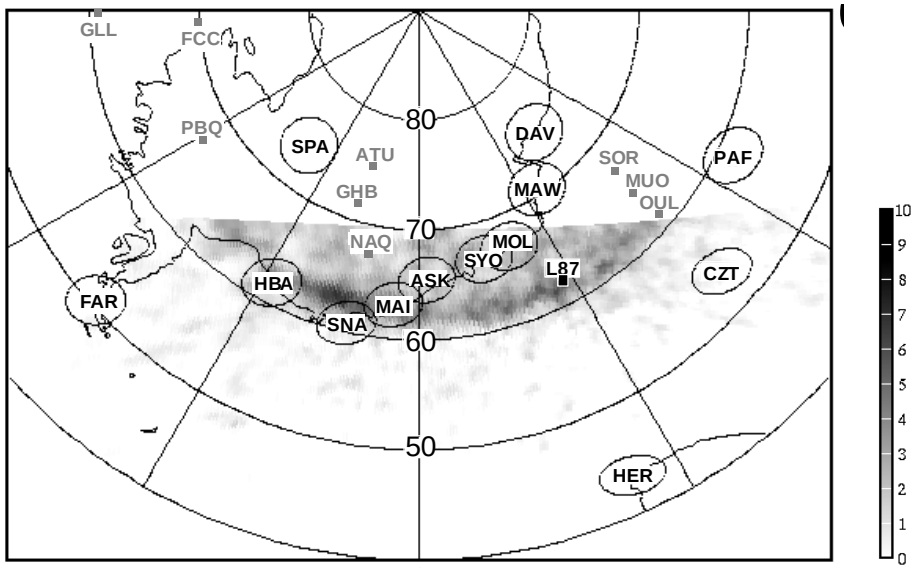

Figure 3.2.1. ATV-UV data at 00:41:44 UT projected at 120 km altitude in the ILAT vs MLT coordinates in the southern hemisphere map. FOV for the elevation above 20 deg at each station is also shown. Foot point of the geosynchronous satellite LANL-1987-097 (L87) is calculated by T89(Kp=5) model. Conjugate locations of some of northern hemisphere stations are shown with gray color.

Figure 3.2.1 shows the spatial relationship between the auroral breakup location and the ground stations. The ATV-UV data at 00:41:44 UT, when the first indication of the breakup was observed, are shown on the southern hemisphere polar map at 120 km altitude in the invariant latitude (ILAT) and MLT coordinates. The auroral emission intensity is shown in the black-and-white scale where a darker region indicates a higher intensity. Breakup occurred near Sanae (SNA) station, and the peak intensity of the brightened area was located at 62.7 deg ILAT and 22.9 hr MLT. The conjugate locations of several stations in the northern hemisphere are shown with a gray color. The field-of-view (FOV) of each station for the elevation above 20 deg, and the foot point location of the geosynchronous satellite, LANL-1987-097 (L87) are also shown. The foot point is calculated by the *Tsyganenko* [1989a] model with Kp=5 (T89(Kp=5)). The meridian scanning photometer (MSP) data at Syowa (SYO) and Asuka (ASK) stations, the all-sky TV data at SYO, the induction magnetometer data at HER, and the magnetometer data from each station in Fig. 3.2.1 are also used in this study.

2.3. Overview of global auroral evolution

After the breakup, the auroral bulge expanded poleward, westward and eastward. The detailed analysis in this study showed that the bulge expansion was not monotonic, but proceeded in a stepwise way. The upper two panels in Fig. 3.2.2 are for the latitudinal and longitudinal intensity profiles of the UV auroral emissions along 23 hr MLT line and 63 deg ILAT line, respectively. The four frame-averaged emission intensity profile is shown at the time of the last frame. The third panel from top is for the total area (black circle) and the total integrated intensity (blank circle) of the UV auroral emissions above a threshold background level within the region of 18-6 hr MLT and 55-80 deg ILAT, and the fourth panel is for the maximum intensity (black circle) and the averaged intensity (blank circle) within the same region. Left and right vertical lines indicate the times of the expansion phase onset and an apparent re-activation of the bulge expansion, respectively.

The latitudinal profile in the top panel shows that the bulge expanded rapidly poleward after the onset. The rapid poleward expansion slowed suddenly around a ceiling latitude of 67 deg ILAT about 2 min after the onset. A further poleward expansion and a further enhancement of the emission intensity re-started around the time of the right vertical line, 00:53 UT, about 11 min after the onset. Looking at the longitudinal profile in the next panel, the bulge expanded predominantly westward during the period of the initial rapid poleward expansion. It suddenly expanded eastward, and then continued to expand slowly both westward and eastward. An apparent acceleration of the azimuthal expansion started around the time of the right vertical line, which is more evident for the eastward expansion. Hence it seems that there were at least three distinct stages in the bulge evolution. The first stage (Stage-1) was characterized by the rapid poleward and westward expansions in a very short

period, and the second stage (Stage-2) was characterized by the slower poleward and azimuthal expansions. In the third stage (Stage-3), both the poleward and azimuthal expansions were accelerated. Looking at each auroral image, as shown later, the Stage-1 was from the onset (00:41:40 UT) to 00:43:43 UT, and the Stage-2 was from 00:45:35 UT to around 00:53 UT. The period between the two stages from 00:43:43 UT to 00:45:35 UT is considered as a transition phase, being characterized by a slow poleward and rapid eastward expansion. The expansion speeds in the poleward, westward, and eastward directions were (2.5, 6.9, 2.6) km/s in the Stage-1, (0.4, 1.9, 5.2) km/s in the transition phase, (0.2, 1.5, 1.0) km/s in the Stage-2, and (1.2, 2.5, 2.8) km/s in the Stage-3, respectively. These expansion speeds were calculated by the shift of the location where the emission intensity was equal to the value of the half width at 00:41:44 UT.

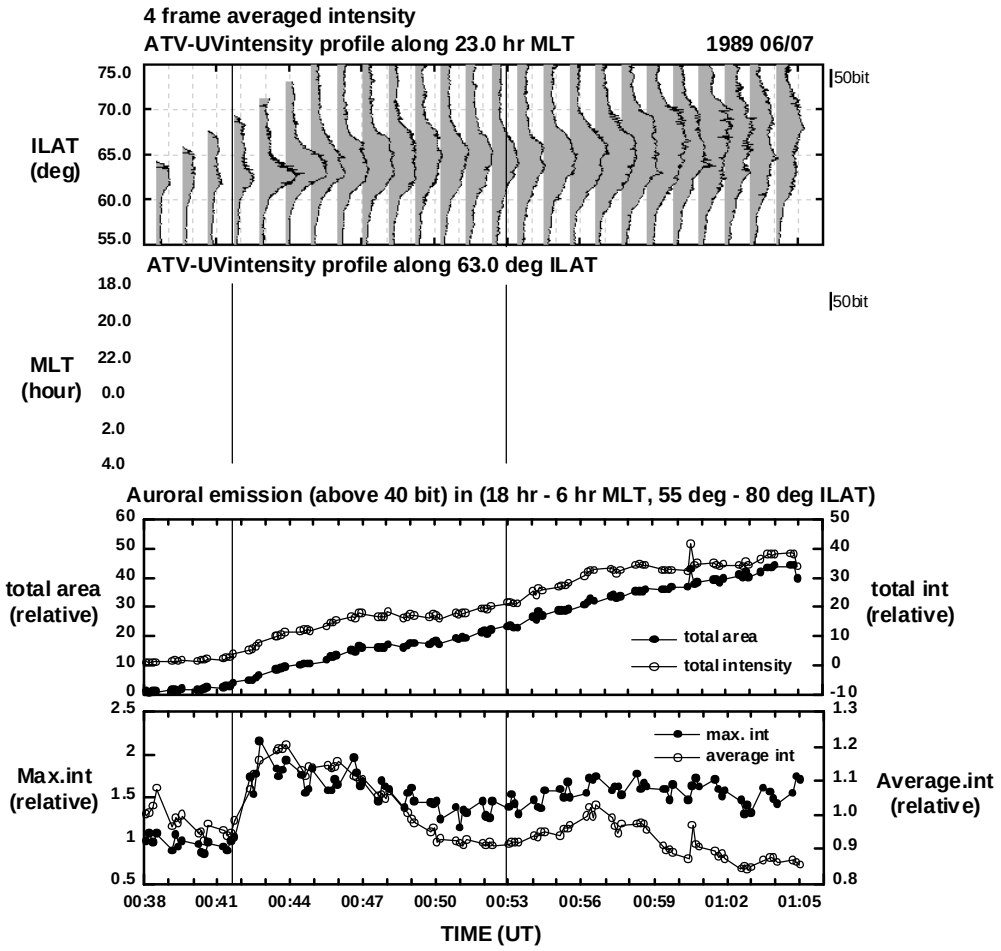

Figure 3.2.2. Auroral bulge evolution observed by ATV-UV from 00:38 UT to 01:06 UT on June 7, 1989. From top: latitudinal profile of the auroral emission intensity along the equi-MLT line at 23.0 hr; longitudinal profile along the equi-ILAT line at 63.0 deg; temporal evolution of the auroral emission, as for the total area (black circle) and total integrated intensity (blank circle); and as for the maximum intensity (black circle) and averaged intensity (blank circle). Parameters in the lower two panels are calculated in the region within 18-06 hr MLT and 55-80 deg ILAT for the emission intensity above a threshold background value (40 bit in original digital value). Left and right vertical lines indicate the times of the expansion phase onset and the apparent re-activation of the bulge expansion at 00:53 UT, respectively.

The lower two panels in Fig. 3.2.2 show that the total, maximum and averaged emission intensities and the total occupied area, all increased rapidly during the Stage-1. During the Stage-2, both the total intensity and total area continued to increase with a smaller increasing rate, while the maximum and average intensities gradually decreased. During the Stage-3, the increasing rates of the total intensity and the total area were enhanced, and the maximum and average intensities started to increase again. Several minutes later, the average intensity turned to decrease. Note that both the maximum and average intensities had their maximum values during the Stage-1.

Figure 3.2.3 shows the evolution of the magnetic activity during the same period as Fig. 3.2.2. The top and bottom panels show the overlaid plots of the amplitude variation of the magnetic horizontal component at the mid- and low-latitude and auroral latitude stations, respectively. The plotted values are the variations from the onset at 00:41:40 UT. The evolution of these magnetic variations are very similar to that of the total emission intensity and the total occupied area of the auroral bulge as shown in Fig. 3.2.2. This suggests that the evolution of the substorm current system should be closely related with the auroral bulge evolution.

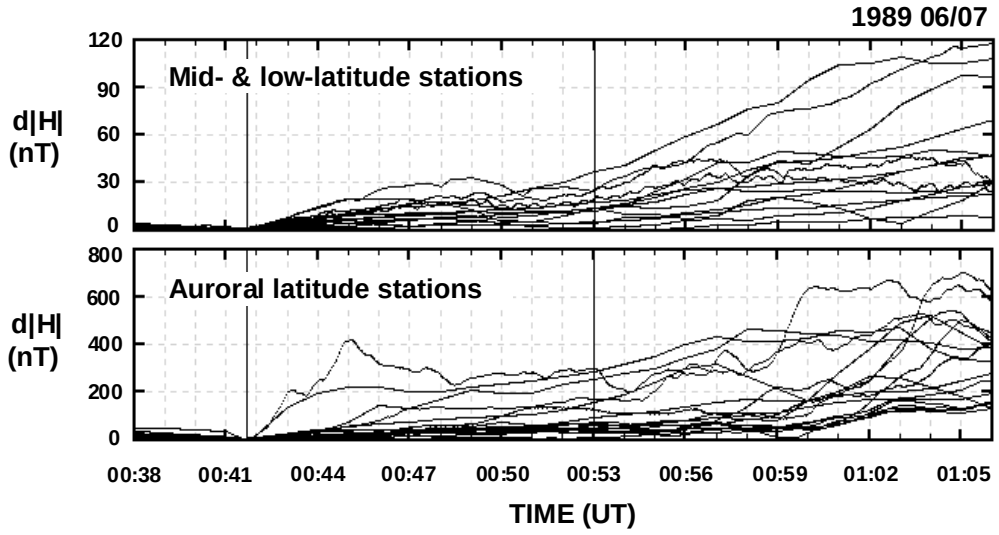

Figure 3.2.3. Magnetic variations from 00:38 UT to 01:06 UT on June 7, 1989. Top and bottom: Overlaid plots of the amplitude variation of the magnetic horizontal component at mid- and low-latitude, and auroral latitude stations, respectively. Left and right vertical lines indicate the times of the expansion phase onset and the apparent re-activation of the bulge expansion at 00:53 UT, respectively.

2.4. Detailed evolution

(1) Timing between the onset phenomena

Figure 3.2.4 shows the detailed evolution of various phenomena from 00:37 UT to 00:47 UT on June 7, 1989. The top four panels are for the magnetic H (northward), D (eastward), Z (downward) components and the 30 MHz riometer output at Halley Bay (HBA).

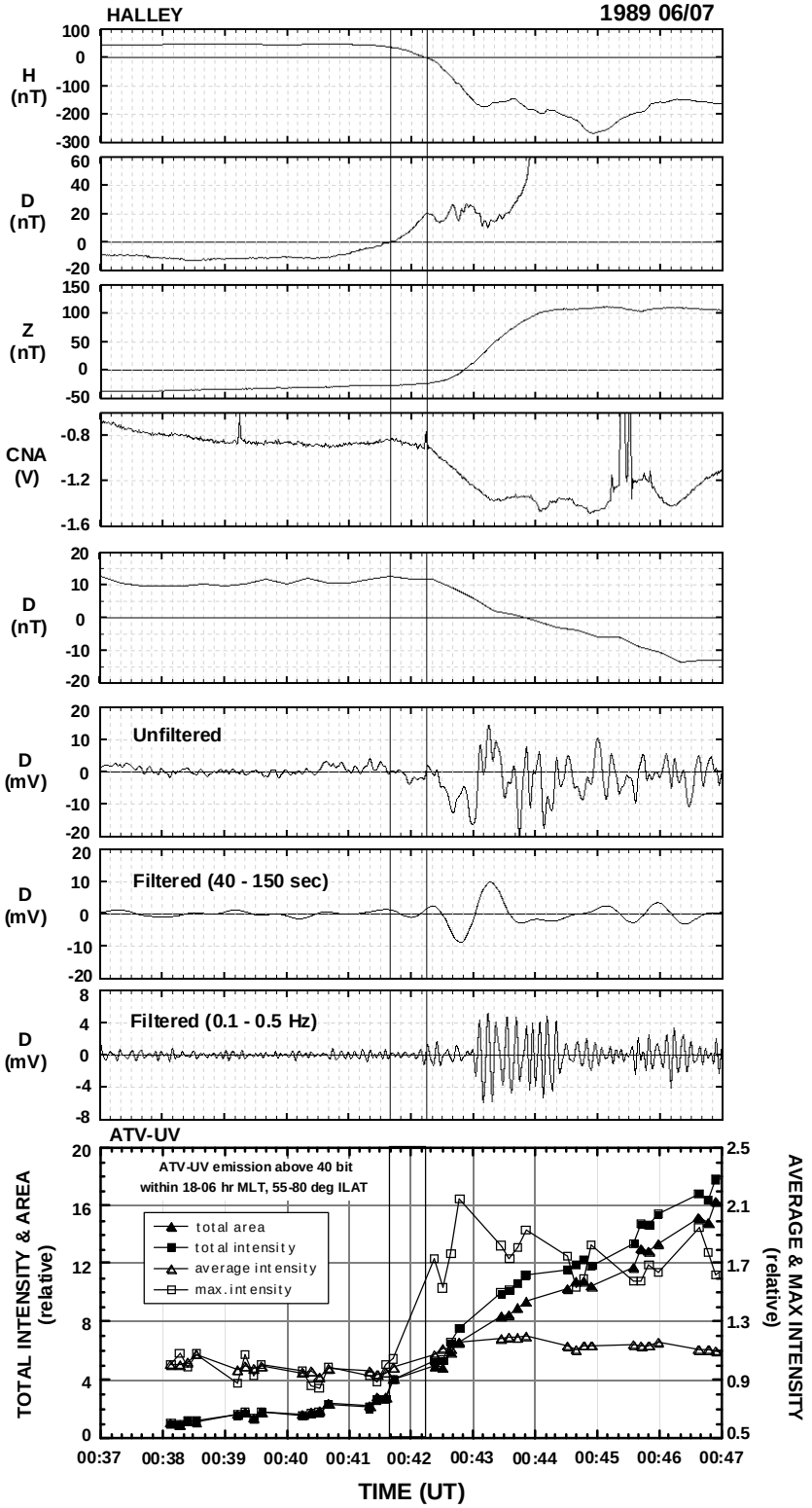

Figure 3.2.4. Observations from 00:37 UT to 00:47 UT. From top: magnetic variations and riometer outputs at Halley; magnetic D-component at Faraday; D-component unfiltered and the Pi2 and Pi1 range band-pass filtered outputs of the induction magnetometer at Hermanus; temporal evolution of the auroral emission observed by ATV-UV, as for the total area (black triangle), total integrated intensity (black square), averaged intensity (white triangle), and maximum intensity (white square). Two vertical lines indicate the time of the expansion phase onset at 00:41:40 UT and the time of an intensification at 00:42:15 UT. See text for detail.

The magnetic variation in the D component at Faraday (FAR) is shown in the next panel. The following three panels are for the D component of the induction magnetometer at HER. Unfiltered and band-pass filtered variations in the Pi2 (40-150 sec) and Pi1 (0.1-0.5 Hz) ranges are shown from the top, respectively. The bottom panel shows the similar parameters of the auroral bulge evolution as in Fig. 3.2.2, within the region of 20-01 hr MLT and 55-70 deg ILAT. The vertical line indicates the time of the expansion phase onset. The temporal resolutions are 1 sec for the data at HBA and HER, and 20 sec for the magnetometer data at FAR.

The onset time of the Pi2 range magnetic pulsation at HER was around 00:41:30-00:41:40 UT [*K. Yumoto*, private communication]. In the bottom panel, all the parameters for the UV auroral emission showed a clear increase from 00:41:44 UT. From these data, we determined the onset time of this substorm as 00:41:40 UT, which is in the range of the estimated Pi2 onset time and is between the ATV-UV observations at 00:41:36 UT and 00:41:44 UT.

About 1 min before the onset, the magnetic H- and D-components at HBA started to decrease and increase, respectively. About 35 sec after the onset (00:42:15 UT), the smooth increase in the D-component at HBA suddenly changed into a more disturbed variation, and the riometer output at HBA showed a rapid increase of the precipitation flux of the energetic electrons. The D-component at FAR also started to decrease, indicating an increase of the upward field-aligned current (FAC) of the substorm current wedge (SCW) system [e.g., *McPherron et al.*, 1973]. The oscillation amplitude of the magnetic pulsations at HER was also enhanced significantly around that time.

From 00:43:40 UT, the D-component at HBA rapidly increased, and the H-component decreased further, which indicates an enhancement of the poleward and westward electrojets. The waveform of the Pi2 pulsation at HER was clear until 00:43:40 UT, and was suddenly damped afterward. The oscillation period of the Pi2 pulsation was about 60 sec. A clear intensification of the Pi1 range pulsations started around 00:43:00 UT, and was damped around 00:44:30 UT.

As already mentioned, the Stage-1 of the auroral bulge evolution lasted until 00:43:43 UT. The transition phase was from 00:43:43 UT to 00:45:35 UT. Comparing with the above mentioned phenomena, the clear waveform of the Pi2 pulsation existed only during the Stage-1, and the Pi1 pulsations started in the middle of the Stage-1 and damped in the middle of the transition phase. The rapid increase of the D-component at HBA occurred during the transition phase. It is not clear that a significant change around 00:42:15 UT was also observed in the auroral bulge evolution, because there was a data gap of 40 sec between 00:41:44 UT and 00:42:24 UT.

(2) Evolution during the Stage-1 and Stage-2

Figure 3.2.5 shows the every auroral image obtained by the ATV-UV from 00:40:40 UT

to 00:46:55 UT in the ILAT vs MLT linear coordinates, mapped at 120 km altitude.

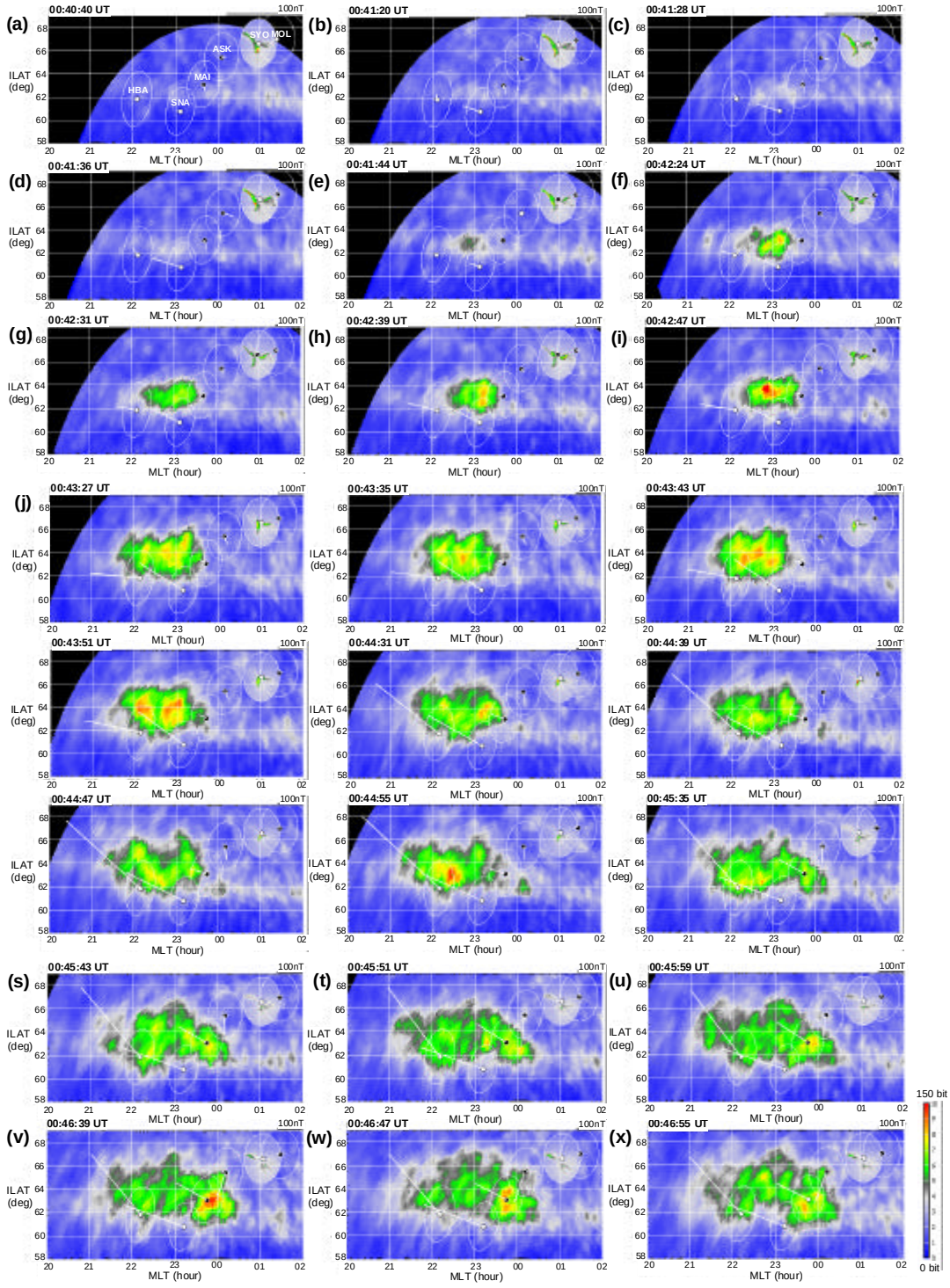

Figure 3.2.5. Every auroral image observed by ATV-UV in the linear ILAT vs MLT coordinates from 00:40:40 UT to 00:46:55 UT on June 7, 1989. White bar with a small circle at each station shows the equivalent current variation vector from 00:40:00 UT for panels (a)-(d) and from 00:41:40 UT for (e)-(x). Auroral activity observed by the all-sky TV camera is shown in the FOV of SYO. White circle at each station indicates the FOV for the elevation above 20 deg.

The color scale for the emission intensity is shown at bottom right corner. The FOV of each station for the elevation above 20 deg is shown with a white circle in each panel. The auroral activity observed by the all-sky TV camera is shown in the FOV of SYO. The white bar with a small circle at each station shows the equivalent current vector, derived by rotating the horizontal magnetic variation vector clockwise by 90 deg. These vectors indicate the deviation from the vectors at 00:40:00 UT for the panels (a)-(d) and at 00:41:40 UT for the panels (e)-(x). The amplitude scale of the magnetic variation is shown at upper right corner in each panel. Note that the scale is different between for panels (a)-(d) and (e)-(x). A black or white circle at each station shows the positive (downward) or negative (upward) variation of the magnetic Z-component, respectively, in the mapping of the northern hemisphere image. The magnetic data are linearly interpolated. The Stage-1 is from panels (e) to (l), the transition phase is from (l) to (r), and the Stage-2 starts from (r).

Prior to the onset, from panels (a) to (d), the equivalent current vectors at HBA and SNA showed an enhancement of the westward electrojet at lower latitudes of the breakup region. A characteristic auroral activity can be seen in the FOV of SYO. As described in the paper-1, on the poleward side of this activity, both the electron and proton auroral emissions, which were observed by the MSP, were quite weak. Since the poleward edge of the 630.0 nm emission is usually considered to be very close to the polar cap boundary [*Blanchard et al.*, 1997], this activity should be located very close to the region of the plasma sheet boundary layer (PSBL). Hence, hereinafter, we call this activity the "NPSBL (Near PSBL) aurora".

The auroral breakup was first identified in panel (e) at 00:41:44 UT. A clear enhancement of both emission intensity and brightening area can be seen in panel (f) at 00:42:24 UT. The westward equivalent currents at both HBA and SNA were also intensified at that time. Judging from the variation of the Z components, the peak of the westward electrojet should be located at higher latitudes of both stations. The auroral bulge expanded rapidly poleward and predominantly westward after that time. This rapid poleward expansion was almost stopped around the time of (l), at 00:43:43 UT. After that time, the poleward expansion continued, but was very slowed. The ceiling latitude of the initial rapid poleward expansion was very close to the latitude of the NPSBL aurora. The complicated form of the NPSBL aurora did not show any remarkable change between before and after the onset (between panels (d) and (e)), and showed a gradual change from the time of (j), at 00:43:27 UT.

The initial rapid westward expansion was slowed around the time of (l). From (m) to (t), the slowed westward expansion proceeded predominantly in the higher latitude part of the bulge. On the other hand, a significant eastward expansion appeared rather suddenly at the time of (r), at 00:45:35 UT, in the lower latitude part of the bulge. After that time (during the Stage-2), the bulge became in a nearly symmetric form, being centered around the meridian of the breakup, and expanded slowly both westward and eastward. The azimuthal expansion first occurred at lower latitudes, and then spread to higher latitudes, which can be seen in the

transition from (r) to (x), more clearly for the eastward expansion.

The most intense emission, all through the expansion phase, appeared in a localized region at the time of (i), at 00:42:47 UT. The emission intensity of the bulge clearly decreased from (m) to (n), and a relatively intense emission region was situated at the eastern part of the bulge from the time of (s). After the time of (x), the emission intensity of the bulge further decreased, especially in its central part (not shown). Both azimuthal parts, especially the eastern part, had a relatively intense emission, which indicates that the energy flux of the precipitating electrons should be larger in the azimuthal parts than in the central part during this period.

It should be noted that the western part of the bulge approached to the rim of the Earth in the FOV of ATV-UV, whereas the eastern part was situated around the center of the Earth during this period. Hence the auroral form of the western part should be less clear due to the larger slant viewing angle from the satellite, compared with the eastern part.

The equivalent current pattern around the bulge was basically unchanged during the Stage-1 (from (e) to (l)), though the current intensity increased. The equivalent current vector at HBA directed westward until the time of (l). During the transition phase (from (l) to (r)), the vector showed a clockwise rotation from westward to more poleward, and its amplitude was enhanced. During the Stage-2, both the direction and amplitude of the equivalent current vector at HBA became stable. The equivalent currents at Maitri (MAI) and ASK also started to develop from (m), showing a clockwise current pattern.

(3) Evolution during the Stage-3

Figure 3.2.6 shows the auroral bulge evolution during the Stage-3 from 00:53:02 UT to 01:04:45 UT with 64 sec (four frame) interval. These are snapshot images at each time. Both local time and latitudinal ranges are larger in Fig. 3.2.6 than those in Fig. 3.2.5. The equivalent current vector at each station in the first panel (a) shows the variation from 00:41:40 UT, and that in the other panels is from 00:53:00 UT. In panel (a), the names of the Antarctic stations are shown. The equivalent current variations at the northern hemisphere stations are also shown in Fig. 3.2.6 in order to look at the evolution of a larger scale equivalent current pattern around the largely expanded bulge. We would not discuss the detailed conjugacy between the northern and southern hemisphere data, but just show how the equivalent current developed in both hemispheres. The foot point location of the L87 satellite, which is calculated with T89(Kp=5) model, is also shown with a white star.

It can be seen in panel (a) that a typical DP1 type [*Nishida*, 1971] equivalent current pattern already developed around the bright auroral region before the start of the Stage-3. An intense westward electrojet flows within the bulge, and its return current can be seen outside of the bulge.

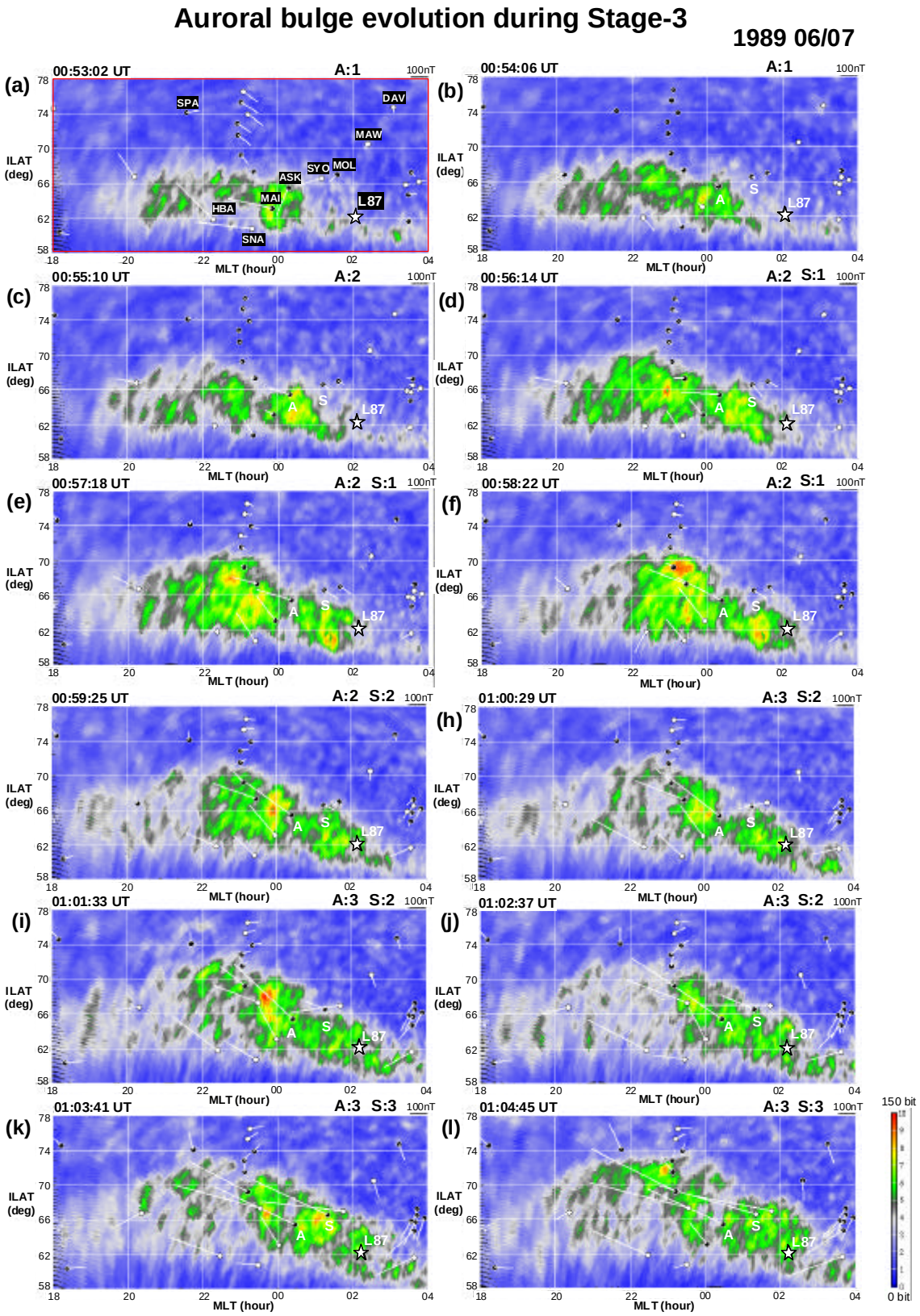

Figure 3.2.6. Auroral bulge evolution observed by ATV-UV in the linear ILAT vs MLT coordinates from 00:53:02 UT to 01:04:45 UT on June 7, 1989 with 64 sec interval. White bar with a small circle at each station shows the equivalent current variation vector from 00:41:40 UT for panel (a) and from 00:53:00 UT for other panels. Equivalent current variation at the northern hemisphere stations is also shown. Foot point location of the L87 satellite, which is calculated with T89(Kp=5) model, is also shown with a white star.

In the next panel (b), an intense emission region appeared around 22-23 hr MLT, extending into higher latitudes, which was a first signal of the further expansion during the Stage-3. The bright region extended also into lower latitudes around that same local time (panel (c)). After that time, the bulge expansion was accelerated both in the poleward and azimuthal directions. The poleward expansion proceeded first around 22-23 hr MLT, and then spread to other local times on both sides. The overall form of the bulge was nearly symmetric in the azimuthal direction, and the local time of the symmetric axis was almost the same as that at the beginning of the Stage-3.

The eastward expansion of the bulge proceeded as follows: it first occurred at lowest latitudes (panel (c)); spread to higher latitudes (panels (d)-(f)); stopped around 66-67 deg ILAT, around the ceiling latitudes of the Stage-1 and Stage-2 (panels (g)-(i)); and then spread further poleward (panels (j)-(l)). This final further poleward expansion at the eastern edge of the bulge started when the eastward front of the further poleward expanding region propagated to that local time.

As the bulge expanded, the emission intensity increased until the time of panel (f), and then decreased. The most intense emission was located in the eastern part of the bulge. Around the central meridian of the bulge, relatively intense emissions can be seen at higher latitudes, as shown in panel (l).

The equivalent current variation in panels (b)-(l) shows that the substorm current system developed further during the Stage-3, simultaneously with the evolution of the auroral bulge. An intense westward and poleward electrojet developed within the bulge, and the return currents developed outside of the bulge. The equivalent current variation at the Greenland west magnetometer network stations, around 23 hr MLT meridian, showed that the flow reversal location from the westward electrojet to the eastward return current gradually moved poleward as the bulge expanded poleward. The optical and magnetic observations at South Pole (SPA) (not shown here) showed that the poleward edge of the bulge reached the zenith of SPA around 01:10 UT and SPA entered the westward electrojet region from the return current region around that time. The poleward edge of the bulge stayed around that latitude until 01:50 UT, and then moved equatorward. SPA went out to the return current region again around 01:55 UT.

The equivalent current variations at SYO and Molodezhnaya (MOL) showed that these stations entered the westward electrojet region around the time of panel (h), from the return current region outside. The flow reversal region was situated around the poleward edge of the bulge. The equivalent current variations at the EISCAT magnetometer cross stations, near 4 hr MLT meridian, showed that the equatorward return currents developed from the time of panel (g), as the bulge expanded eastward and approached to the stations.

(4) Observations at Asuka and Syowa stations

Figure 3.2.7 shows the MSP data at ASK from 00:40 UT to 01:20 UT on June 7, 1989. The MSP observed three auroral emission lines (OI (557.7 nm, 630.0 nm) and Hß (486.1 nm)) along the magnetic meridian with the scanning speed of 30 sec from horizon to horizon. We assumed the emission altitudes of 120 km for 557.7 nm and Hß emissions, and 250 km for 630.0 nm emission to make the intensity ILAT profile.

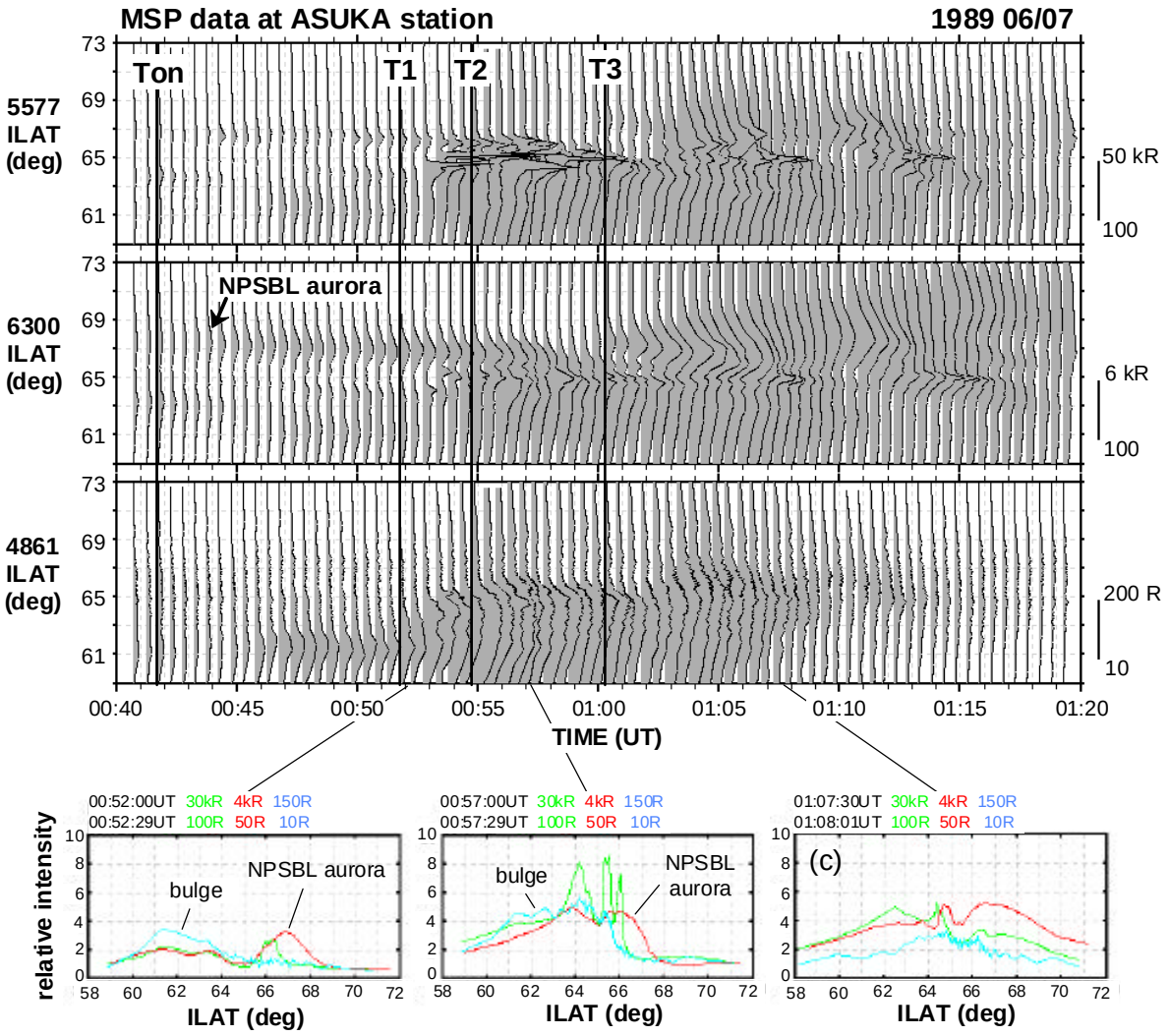

Figure 3.2.7. MSP data at ASK. Top panel: ILAT vs time plot of the three auroral emission lines (557.7 nm, 630.0 nm, 486.1 nm) from 00:40 UT to 01:20 UT on June 7, 1989. Four vertical lines indicate the time of the expansion phase onset (Ton), and the start times of the local first stage (T1), second stage (T2), and third stage (T3), respectively. Bottom panels: Intensity ILAT profiles of the three emission lines at three selected times. Green, red, and blue lines are for 557.7 nm, 630.0 nm, and 486.1 nm emissions, respectively. Scanning start and end times, and the maximum and minimum intensities (in Rayleigh) for the three emission lines, corresponding to the vertical axis, are shown on the top of each panel.

In the MSP data, the eastward expansion of the lower latitude part of the bulge can be identified as an intensity enhancement around 62 deg ILAT both in the electron and proton emissions from around 00:46 UT. A latitudinal confined electron auroral activity around

66-68 deg ILAT, which is most clearly seen in the 630.0 nm emission, is the NPSBL aurora. The NPSBL aurora existed before the onset, and was intensified about 2-3 min after the onset. A clear poleward expansion of the bulge started around 00:51:45 UT (T1). The poleward expanding bulge approached the NPSBL aurora, and was almost in contact with it around 00:54:44 UT (T2). The poleward expansion almost stopped after that time. From about 2 min before the contact, a very intense discrete auroral activity appeared in the 557.7 nm data at the poleward edge of the bulge. After T2, the intensity of the NPSBL aurora was enhanced until 00:57:15 UT, and then decreased. Its peak location gradually moved equatorward.

A further poleward expansion started around 01:00:15 UT (T3), which is most evident in the 630.0 nm data. The further expansion started with a significant intensification of the auroral activity in the most poleward region, separated from the main body of the bulge on the lower latitude side. That activity appeared at higher latitudes of the previous NPSBL aurora and became the poleward-most auroral activity. After T3, the location of the intensity peak of that activity gradually moved equatorward, whereas its latitudinal width significantly increased. An intensity gap appeared between the poleward-most region and the enhanced emissions on the equatorward side. The equatorward part gradually moved equatorward, which is evident in the 557.7 nm data. Hence a latitudinal bifurcation of the electron emission occurred after the further poleward expansion. In the poleward-most region, the proton emission was relatively weak, whereas in the equatorward region, both the electron and proton emissions coexisted. As time progressed, the proton emission gradually became weak, and eventually almost disappeared in the whole latitudinal range. Such a fading of the proton auroral emission occurred from lower latitudes.

In summary, the detailed observation by the MSP showed that the local poleward expansion also had characteristic stages in its evolution. The first stage was from T1 to T2 in Fig. 3.2.7, the second stage was from T2 to T3, and the third stage was after T3. The latitudinal evolution in these three stages in the local observation is very similar to that in the Stage-1 to Stage-3 in the global auroral evolution. The transition phase in the global evolution, which was characterized by a very slow poleward and rapid eastward expansion, was not clear in the one-dimensional local observation.

The latitudinal intensity profiles at selected times during the three local stages are shown in the bottom three panels in Fig. 3.2.7. In each panel, abscissa is ILAT from 58 to 72 deg, and ordinate is the relative emission intensity of the three auroral emission lines. The intensity profiles of the 557.7, 630.0, and 486.1 nm emissions are shown with green, red, and blue lines in each panel, respectively. During the local first stage (panel (a)) and the second stage (panel (b)), both the electron and proton emissions coexisted in the auroral bulge on the equatorward side. After the bifurcation of the electron emission region during the local third stage (panel (c)), the intensity ratio, 557.7/630.0, in the equatorward region was higher than that in the poleward region. This suggests that the characteristic energy of the precipitating electrons in

the equatorward region should be higher than that in the poleward region.

The similar stepwise evolution of the auroral poleward expansion was also observed by the MSP at SYO with a time delay of 3-4 min from ASK (not shown here). The start times of the local three stages were 00:55:31 UT (T1), 00:59:01 UT (T2), and 01:03:01 UT (T3), respectively. The characteristics of the three stages were also very similar. The all-sky TV data at SYO showed that the poleward expansion proceeded as a stepwise poleward shift of an azimuthally extended bright region (not shown here). An intense discrete auroral activity, which appeared during the local second stage, had a ray-structure and also extended azimuthally. After T3, the bright region spread in the whole FOV, and the ray-structured form appeared within it. The pulsating auroral activity appeared in the equatorward part of the bright region around 01:09 UT, and developed afterward. The ray-structured activity changed into the more diffuse one afterward. Such auroral activities as the WTS or the N-S aurora, which can be usually seen in the expansion at the western edge of the bulge [e.g. *Nakamura et al.*, 1993], were not identified.

Comparing with the ATV-UV data in Fig. 3.2.6, the transition from the local first stage to the second stage at ASK and SYO occurred between panels (b) and (c) in Fig. 3.2.6, and between (f) and (g), respectively. The stages of the local evolution at ASK and SYO are shown on the top of each panel in Fig. 3.2.6 as "A:2" and "S:2", respectively. The transition from the local second stage to the third stage at ASK and SYO occurred between panels (g) and (h), and between (j) and (k), respectively. The start of the local third stage at each station was nearly coincident with the arrival of the further poleward expanding region of the global auroral bulge during the global Stage-3.

(5) Observation at geosynchronous orbit

Figure 3.2.8 shows the flux variation of the energetic electrons and ions observed by the L87 from 00:30 UT to 01:20 UT on June 7, 1989. The foot point of the L87 satellite was located about 1 hour later from SYO, as can be seen in Fig. 3.2.1. Temporal resolution of the L87 data was about 1 min.

The number flux of the energetic electrons started to increase around 00:53 UT (FT1) over a broad energy range. The increasing rate decreased from 00:58 UT (FT2) to 01:03 UT (FT3). Further increase started from FT3 or 1 min later. The enhanced flux was maintained after that time. These flux variations occurred in almost dispersionless way, at least with the 1 min resolution. The six horizontal bars around 01:00 UT indicate the values at 23:40 UT on June 6, 1989 for the six energy ranges, when the flux started to decrease at the beginning of the growth phase. It can be seen that the flux levels from FT2 to FT3 were nearly equal to the initial levels. The number flux of the energetic ions also showed the similar variation. In summary, the increase of the number flux of the energetic particles also showed a stepwise evolution.

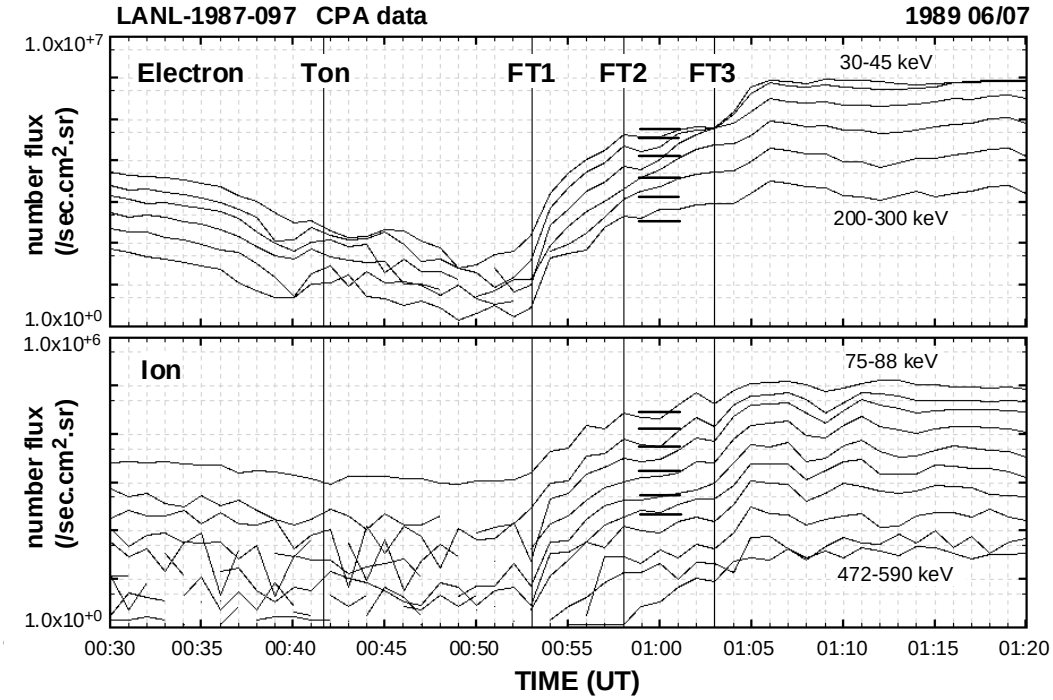

Figure 3.2.8. Flux variation of the energetic electrons (top panel) and ions (bottom panel) observed by L87 from 00:30 UT to 01:20 UT on June 7, 1989. Horizontal bar around 01:00 UT in each panel indicates the pre-growth phase level at 23:40 UT on June 6, 1989 for each energy range. Onset time of the expansion phase (Ton), and three specific times in the flux increase, FT1, FT2, and FT3, are indicated with vertical lines.

Looking at the ATV-UV data in Fig. 3.2.6, the first rapid flux recovery from FT1 to FT2 occurred before the eastward front of the bulge reached the local time of L87 (from the panel (a) to (f)). In other words, this initial flux increase preceded a significant enhancement of auroral particle precipitation. The second gradual flux increase from FT2 to FT3 occurred when the foot point of L87 was included well within the bulge, but eastward expansion of the further poleward auroral region did not reach that local time yet (from (f) to (j)). Finally, the further flux increase after FT3 occurred after the further poleward region expanded eastward beyond the local time of L87 (from (k) to (l)). Such a flux variation should be related with both the configuration change (dipolarization) of the magnetic field lines and the actual earthward transport of the newly injected particles in the magnetosphere. The observations by L87 suggest that the increase from FT1 to FT2 should be mainly caused by the configuration change without significant injections, and the further increase after FT3 should be related with both the dipolarization and the injections.

Note that if we use the T89(Kp=0) model for the field line tracing, the foot point location of L87 is about 65.9 deg ILAT and 2.2 hr MLT at 00:58 UT, hence the latitude is shifted-up by about 3.8 deg whereas the local time is nearly the same as that in the case of the T89(Kp=5) model. We have also tried the model by *Tsyganenko* [1996] and found that the local time of the foot point was nearly the same as that in the case of the T89 model.

3. Observation summary and Discussions

3.1. Observation summary

Figure 3.2.9 schematically shows our view for the evolution of the auroral bulge and the substorm current system in this event. Black arrow with a triangle head shows the expansion direction of the auroral region. The estimated locations of the positive and negative ionospheric potentials are shown with the plus and minus signed areas, respectively. Light and dark areas within the bulge indicate weak and intense emissions, respectively.

It was found that there were three distinct stages in the auroral bulge evolution.

The Stage-1 was characterized by the rapid poleward and rapid azimuthal (predominantly westward) expansions in a short time (about 2 min) (Fig. 3.2.9(a) and (b)). The poleward expansion suddenly slowed around the latitudes of the NPSBL aurora, which appeared a few minutes before the onset and continued to exist near the ionospheric PSBL region. During this stage, both the maximum and average emission intensities rapidly increased and reached their maximum values.

There was a certain period for the transition from the Stage-1 to the Stage-2, which was characterized by the very slow poleward and rapid eastward expansions (Fig. 3.2.9(c)). The emission intensity of the NPSBL aurora was enhanced during the transition phase.

The Stage-2 was characterized by the very slow poleward and slower and continuous azimuthal expansions (Fig. 3.2.9(d)). Both the maximum and average intensities gradually decreased during this stage. As the bulge expanded, the emission intensity in its central part gradually became weak, comparing with its eastern and western sides. The azimuthal expansion first occurred at lower latitudes, and then spread to higher latitudes.

The Stage-3 was characterized by a sudden acceleration of both the poleward and azimuthal expansions. The accelerated poleward expansion proceeded first around the initial onset local time, and then spread to other local times on both sides (Fig. 3.2.9(e)-(g)). The overall form of the bulge was nearly symmetric from the beginning of this stage. As the expansion proceeded, both the maximum and average intensities increased first, and then decreased. The emission intensity in the central part gradually decreased, and a relatively intense emission appeared in the eastern part and at the higher latitudes of the central part (Fig. 3.2.9(g)).

The substorm current system started to develop soon after the onset (Fig. 3.2.9(a) and (b)), and its further significant evolution was observed during the transition phase (Fig. 3.2.9(c)). During the Stage-2, the evolution of the current system became stable. The westward and poleward electrojet developed within the bulge, and its return currents developed outside of the bulge, which suggests that the negative and positive ionospheric potentials were located at the equatorward-westward and poleward-eastward sides of the bulge, respectively. Such an equivalent current pattern expanded azimuthally simultaneously with the azimuthal expansion of the bulge (Fig. 3.2.9(c) and (d)). The further evolution of the current system started

simultaneously with the start of the Stage-3. The westward and poleward electrojet and its return currents further developed within and outside of the bulge, respectively. The demarcation region between the electrojet and the return currents was located around the boundary of the bulge, and moved in the poleward and azimuthal directions simultaneously with the poleward and azimuthal expansions of the bulge (Fig. 3.2.9(e)-(g)).

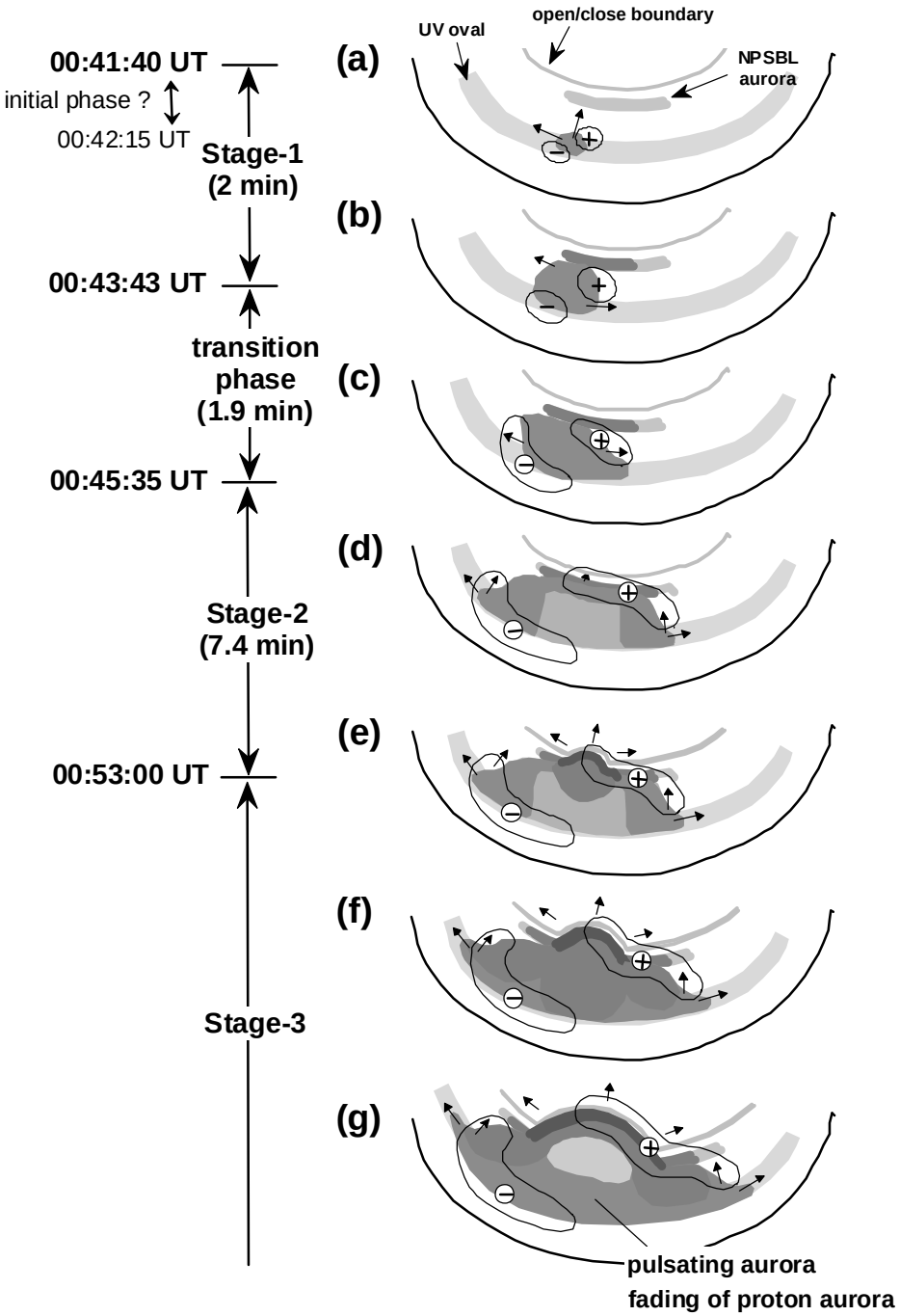

Figure 3.2.9. Schematic summary of the evolution of the auroral bulge and the substorm current system in this event. Darker area represents an intense emission region of the bulge, and the plus (minus) signed area shows a central part of the positive (negative) ionospheric potential region.

The local expansion at the azimuthal front also showed a three-stage evolution similar to the global evolution. From the simultaneous observations of the global and local evolutions, it can be supposed that the global expansion during the Stage-3 should proceed as a continuous azimuthal propagation of such a local three-stage evolution. From this point of view, the poleward expansion at the initial onset meridian should also proceed in the same way as observed at ASK and SYO. The proton auroral emission should coexist with the electron emission within the bulge during the Stage-1 and the Stage-2 in Fig. 3.2.9(a)-(e), an intense electron auroral activity should appear at the poleward edge of the bulge during the transition phase and the Stage-2 in Fig. 3.2.9(b)-(e), and the further poleward expansion during the Stage-3 in Fig. 3.2.9(e) should start with the significant intensification of the poleward-most activity. The bifurcation of the electron emission region should occur in Fig. 3.2.9(e)-(g). The fading of the proton auroral emission should occur, and the pulsating auroral activity should appear in the equatorward region of the central part of the bulge in Fig. 3.2.9(g).

In this event, the Pi2 onset almost coincided with the auroral breakup, as shown in Fig. 3.2.4. About 35 sec after the onset during the Stage-1, a clear intensification was observed in the amplitude of the Pi2 pulsation, the substorm current system, and the energetic electron precipitation, and a sudden change was observed in the magnetic D-component variation at HBA. A clear waveform of the initial Pi2 pulsation was observed only during the Stage-1, and was significantly damped afterward. A significant intensification of the Pi1 pulsations started during the Stage-1 about 45 sec after the intensification of the Pi2 amplitude, and damped in the middle of the transition phase.

3.2. Comparison with previous observations

As discussed in the introduction section, such a stepwise evolution of the auroral bulge as shown in this study seems to be a common feature which is frequently observed during the expansion phase of a substorm. However, to our knowledge, there are very few previous works showing clearly a full process of such a systematic stepwise evolution of the auroral bulge and pointing out its importance in the context of magnetospheric substorm. We have analyzed both the satellite global auroral images and the ground-based optical observations, together. Previous works mainly depend on only the ground-based data [e.g. *Akasofu*, 1964; *Montbriand*, 1971] or only the satellite-based data [e.g. *Rostoker et al.*, 1987b; *Hones et al.*, 1987]. One of our new findings is that such a stepwise evolution also occurred locally at the azimuthal front of the global auroral bulge, and the azimuthal expansion of the global bulge can be understood as a successive propagation of such a local stepwise evolution. To study such a process, the simultaneous observations of the global and local auroral evolutions were essentially important.

It is also newly found that the NPSBL aurora (or poleward-most auroral activity) should play an important role in the stepwise evolution of the auroral bulge. *Shepherd and Murphree*

[1991] showed an example where a rapid poleward expansion of the bulge was stopped around the latitudes of a pre-existing arc about 1 min after the onset. Such a rapid poleward expansion of the initial bulge toward the pre-existing polar arcs was also pointed out by *Frank and Sigwarth* [2000]. Such a pre-existing arc could be the NPSBL aurora in our event. Previous studies also showed that a further poleward expansion started with an intensification of the higher latitude side of the central part of the bulge [e.g. *Henderson et al.*, 1998; *Rostoker et al.* 1987b], which should correspond to the start of the Stage-3 with a significant intensification of the poleward-most activity in our event. Those previous studies also showed that the "double oval" configuration clearly appeared only after the further poleward expansion, which should correspond to the bifurcation of the electron emission region after the further poleward expansion during the local third stage in our event.

The proton auroral emission coexisted with the electron emission within the bulge during the local first stage to the second stage in this event. This is consistent with the observation by *Takahashi and Fukunishi* [2001], who showed that both emissions coexist within the poleward expanding bulge especially in the initial stage. Previous studies showed that the equatorward boundary of the proton auroral region rapidly moved poleward within a well-developed auroral bulge, and such a poleward motion frequently occurred simultaneously with the appearance of the N-S auroras [*Montbriand*, 1992; *Fukunishi*, 1975b; *Takahashi and Fukunishi*, 2001]. In our event, the fading of the proton auroral emission occurred from the lower-most latitudes, and spread to the higher latitudes during the local third stage, which should correspond to those previous observations. The N-S auroras could not be identified in the FOV of the ground stations in our event, because we observed the poleward expansion at the eastern side of the bulge. It should be emphasized again that the above mentioned evolution in the proton auroral activity was closely related with the stepwise evolution of auroral bulge.

The substorm current system also showed a stepwise evolution associated with the evolution of the auroral bulge. During the Stage-3, the intense electrojet region rapidly expanded poleward simultaneously with the rapid poleward expansion of the bulge, which should correspond to the intensification of the electrojet at the most poleward region in *Kisabeth and Rostoker* [1971] and the further large-scale poleward shift ("poleward leap") of the electrojet in *Pytte et al.* [1976b] or *Hones et al.* [1970; 1984].

Such a good coincidence between the initial rapid poleward expansion of the bulge and a clear waveform of the initial Pi2 as shown in this event can be seen in previous studies [e.g. *Liou et al.*, 1999 (in their Plates 3 and 4)]. The delayed start of the significant Pi1 pulsations from an intensification of the initial Pi2 pulsation can also be seen in previous studies both in the magnetosphere (Fig. 3.2.1 of *Sakurai and McPherron* [1983]; Fig. 3.2.2 of *Saka et al.* [1996]) and on the ground (Fig. 3.2.2 of *Bösinger and Wedeken* [1987]; Fig. 3.2.1 of *Yumoto* [1990]).

3.3. Evolution in the magnetosphere

As discussed in detail in the paper-1, the NPSBL aurora should be closely associated with some process around an X-type neutral line in the tail, and the characteristics of its evolution suggest that the neutral line should be the near earth neutral line (NENL). It has been well-established from the observations by the GEOTAIL satellite that the NENL is actually formed during the substorm evolution [e.g., *Ieda et al.*, 1998], and its initial location should be around X=-20 to -30 Re [e.g., *Nagai et al.*, 1998; *Nagai and Machida*, 1998; *Machida et at.*, 1999; *Miyashita et al.*, 2000]. The auroral substorm evolution observed in this event seems to be well-fitted in the frame of those previous studies in many aspects.

It is a critical issue whether the initial formation of the NENL occurs before or after the expansion phase onset. The NPSBL aurora appeared a few minutes before the onset, which seems consistent with the previous event studies and statistical studies suggesting that the initial formation of the NENL starts about 1 to 5 min before the ground-based Pi2 onset [e.g. *Nagai and Machida*, 1998; *Machida et al.*, 1999; *Miyashita et al.*, 2000]. The NPSBL aurora was intensified during the transition phase and the Stage-2 about 2-3 min after the onset, which is also consistent with their results showing that the fast earthward and tailward flows from the NENL are clearly enhanced soon (about 1-2 min) after the Pi2 onset.

The Stage-3 started about 11 min after the onset, which should correspond to the statistical results by *Machida et al.* [2000], who showed that a clear enhancement of the tailward flows appears in the mid-tail region about 10 min after the onset. They also showed that the earthward flows originating from the distant neutral line disappear about 10 min after the onset. These observations suggest that the lobe field line reconnection should start at the NENL around that time.

The latitudinal location of the NPSBL aurora was almost unchanged during the local first stage, and its peak location moved equatorward during the local second stage. During the local third stage, another poleward-most activity appeared at higher latitudes of the previous NPSBL aurora, and its poleward edge rapidly expanded poleward. These observations suggest that the configuration of the field line threading from the poleward-most activity should not be suffered a significant dipolarization during the Stage-1 and Stage-2, and its significant dipolarization should occur soon after the start of the Stage-3. *Baumjohann et al.* [1999] showed that the magnetic configuration in the innermost region (-11>X>-16 Re) becomes the most dipolar one about 15 min after the onset, and the dipolarization propagated gradually tailward with a speed of about 35 km/s. *Asano et al.* [1998] also showed a slow tailward propagation of the dipolarization with about 30 km/s. *Baumjohann et al.* [1999] also showed that the dipolarization reaches the NENL location (around -21>X>-26 Re) about 45 min after the onset.

Comparing with such a slow tailward propagation of the dipolarization in the later stage

of the substorm, the initial poleward expansion during the Stage-1, which occurred within 2 min, was very rapid. This initial rapid poleward expansion could be associated with the rapid tailward propagation of the current disruption (CD) with a speed of about 150-300 km/s in the tail, as shown by *Jacquey et al.* [1991; 1993] and *Ohtani et al.* [1992a]. It can be supposed that during the Stage-1 in this event, such CD should proceed in the closed field line region earthward from the NENL, and should not cause the significant configuration change of the field line threading from the NENL. Hence the CD (or dipolarization) process during the Stage-1 should be different in its characteristics from that in the later stage during the Stage-3. In the CD model, a rarefaction wave is launched tailward from the near earth onset region after the onset [e.g., *Lui*, 1991a]. The propagation speed of the rarefaction wave should be that of the fast mode wave in the tail, which could be comparable with or larger than the propagation speed of the CD of *Jacquey et al.* [1991; 1993] or *Ohtani et al.* [1992a] [cf., *Moore, et al.*, 1987]. The initial rapid poleward expansion during the Stage-1 could be associated with the rapid tailward propagation of a rarefaction wave that is closely related with the CD and dipolarization process in the tail.

The Pi2 pulsations are considered to be an odd-mode fundamental oscillation of the geomagnetic field lines anchored at the onset location in the ionosphere [*Kuwashima and Saito*, 1981; *Takahashi et al.*, 1992]. *Yumoto et al.* [1989] showed that some of Pi1 pulsations also showed an odd-mode oscillation of the geomagnetic field line as in the case of the Pi2. Hence both the Pi2 and Pi1 pulsations should be associated with some magnetospheric processes which excite such oscillations of the magnetic field lines, and the time delay between both pulsations suggests the time delay between two responsible processes operating in the magnetosphere. The good coincidence between the initial rapid poleward expansion of the bulge and the clear waveform of the initial Pi2 suggests that the magnetospheric process for the Pi2 should be closely related with the initial rapid tailward propagation of the CD or the rarefaction wave.

The distinct changes about 35 sec after the onset in the ground magnetic variation and the energetic particle precipitation suggest that some distinct changes should occur in the magnetosphere at that time. Assuming the odd-mode fundamental oscillation, the propagation time of the hydromagnetic wave in the Pi2 range, from the equatorial source region to the ionosphere, should be a quarter of the oscillation period, about 15 sec in this event. The 35 sec is about two times of the propagation time. The Pi2 wave related with the expansion phase onset should be launched in the magnetosphere about 15 sec before the ground Pi2 onset. Hence the distinct changes were observed about three times of the propagation time after the initial generation of the Pi2 wave in the magnetosphere. In other words, the hydromagnetic wave experienced one bounce and one way between the equatorial plane and the ionosphere before the distinct changes were observed on the ground. Note that the traveling time of the energetic (>30 keV) electrons from the equatorial plane to the ionosphere should be much

shorter (less than 1 sec) than that of the hydromagnetic wave.

The substorm current system showed a clear further development during the transition phase and the Stage-3. The MHD simulation by *Birn and Hesse* [1996] and *Birn et al.* [1999] showed that the FACs in the SCW system are produced in the near earth region as a result of the magnetic and plasma flux transports by the enhanced earthward flows from the NENL and their braking and azimuthal deflection. The further development of the substorm current system indicates a further development of the fast earthward flows, hence, a further enhancement of the reconnection rate at the NENL.

In the CD model, the FACs in the SCW system are a consequence of the disruption of the cross-tail current due to the magnetic field turbulence caused by some kinetic instability, and do not require the fast earthward flows from the NENL [e.g., *Lui*, 1996]. As discussed above, the auroral evolution during the Stage-1 seems to be fitted better in the frame of the CD model. Hence the development of the SCW system during the Stage-1 could be associated with such a process in the CD model.

The poleward part of the bifurcated electron emission region during the local third stage should be closely associated with the reconnection process at the NENL, whereas the equatorward part should be associated with the electron injection into the near earth region. Injected electrons should move eastward mainly by the magnetic drift, and precipitate into the ionosphere due to some pitch-angle scattering processes, causing the pulsating auroras [e.g. *Davidson*, 1979; *Johnstone*, 1983]. The duration of the equatorward motion of the electron emission region after the bifurcation was rather short, about 15 min, which suggests that a significant injection should occur in the close vicinity of the azimuthally expanding front, not in the whole disturbance region. This interpretation is consistent with those by *Nakamura et al.* [1991] and *Arnoldy and Moore* [1983].

One of the main precipitation mechanisms for the plasma sheet protons is considered to be the non-adiabatic pitch-angle scattering around the highly curved equatorial plane [e.g. *Sergeev et al.*, 1993a]. The transition from the non-adiabatic to adiabatic motion strongly depends on the relationship between the magnetic field line curvature and the particle gyroradius [e.g. *Büchner and Zelenyi*, 1989]. When a significant dipolarization occurs, the field line curvature increases, the proton motion becomes more adiabatic, and the pitch-angle distribution should become more trapped one due to the conservation of the first adiabatic invariant. Such a change in the pitch-angle distribution of the ions was actually observed at geosynchronous orbit [e.g. *Sauvaud and Winckler*, 1980]. Hence the precipitation of the protons should become extremely weak in such a significant dipolarization region. In our event, the proton auroral emission almost disappeared in the whole latitudinal range after the bifurcation of the electron auroral emission during the local third stage. This observation suggests that a significant dipolarization should occur within the disturbance region in the magnetosphere during that period. The further flux increase of the energetic particles after

FT3 in Fig. 3.2.8 also indicates that such a significant dipolarization should occur at geosynchronous orbit during that period.

The precipitation mechanism for the protons during the local first stage to the second stage should be different from the above mentioned non-adiabatic pitch-angle scattering, because the enhancement of the proton emissions appeared simultaneously with the enhancement of the electron emissions within the bulge. *Chen et al.* [2000] showed that both energetic electrons and ions were accelerated along the magnetic field lines at geosynchronous orbit about 1-2 min after the onset. The Fermi acceleration due to the rapid dipolarization (fast earthward flows) could be a possible mechanism for such charge-independent acceleration [cf. *Delcourt et al.*, 1990].

Figure 3.2.10 shows our schematic view for the evolution in the magnetospheric X-Y (left row) and X-Z (right row) planes during the expansion phase of this event, which is based on the above discussions. The seven panels in Fig. 3.2.10 correspond to the ionospheric evolution shown in the seven panels in Fig. 3.2.9, respectively.

After the onset in the magnetosphere, the tailward stretched field lines start to move earthward to become a more dipolelike configuration, which means the start of a field line oscillation in the radial direction, hence the trigger of a fundamental odd-mode and compressional mode poloidal oscillation of the Pi2. This configuration change should be triggered by a sudden breakdown of the stress balance between the plasma pressure gradient, magnetic pressure gradient, and the magnetic tension in the near earth localized region.

An effective field-aligned acceleration of the plasma (both ions and electrons) occurs in association with this earthward motion, which causes the auroral breakup in the ionosphere (Fig. 3.2.10(a)). Such an earthward motion of the plasma propagates tailward as a fast mode rarefaction wave, which means that the source region of the initial bulge spreads tailward with a speed of the fast mode wave.

The NENL formation starts a few minutes before the onset, and the source region for the NPSBL aurora is located at the earthward vicinity of the NENL. The initial dipolarization during the Stage-1 occurs on the closed field lines earthward of the NENL.

When the initial rarefaction wave reaches the NENL location, the reconnection rate at the NENL increases. The enhanced earthward flows can transport a larger amount of the plasma and magnetic fluxes into the near earth region, which causes the start of a significant development of the SCW system. This is the start of the transition phase (Fig. 3.2.10(b)). Since the fast flows should be bursty and spatially localized [e.g. *Angelopoulos et al.*, 1992; 1997], they should cause a magnetic field turbulence in a higher frequency range and in a shorter wavelength compared with the Pi2 oscillations [e.g. *Fairfield et al.*, 1999]. Such a turbulence should perturb the Pi2 oscillations, and could be the source of the enhanced Pi1 pulsations observed at the ground. The reconnection rate decreases at the end of the transition

phase (Fig. 3.2.10(c)). The magnetic field turbulence is damped, and the evolution in the magnetosphere moves into a more steady state after that time.

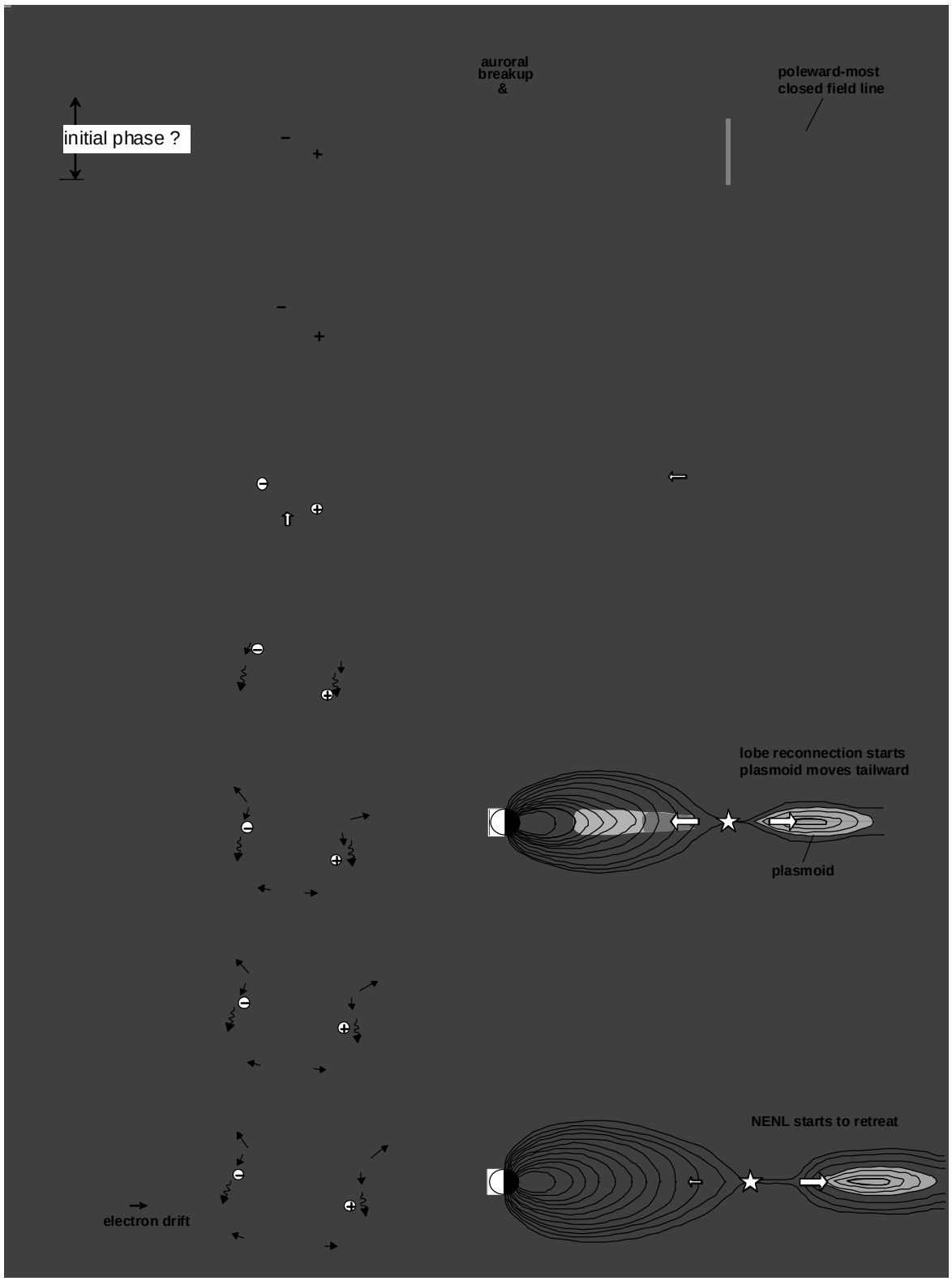

Figure 3.2.10. Schematic view of the evolution in the magnetospheric X-Y (left row) and X-Z (right row) planes during the expansion phase of this event. Seven panels correspond to the ionospheric evolution shown in the seven panels in Fig. 3.2.9, respectively.

During the Stage-2, the slow dipolarization continues in the central part of the disturbance region due to the slow reconnection of the plasma sheet field lines at the NENL. Whereas, the similar process from the Stage-1 to the transition phase occurs locally at both azimuthal fronts of the disturbance region. The azimuthal expansion of the disturbance region proceeds as a result of the successive propagation of such a local process (Fig. 3.2.10(d)).

When the reconnection process at the NENL reaches the field lines in the lobe region, the reconnection rate increases significantly. This is the start of the Stage-3 (Fig. 3.2.10(e)). The lobe field line reconnection first starts around the local time of the initial onset. The enhanced fast earthward flows cause a significant dipolarization in the disturbance region, a further development of the SCW system and an enhanced auroral particle precipitation. The lobe field line reconnection starts later at the other local times on both sides, hence the lobe reconnection region expands in the azimuthal direction along the NENL (Fig. 3.2.10(f)).

The enhanced magnetic and plasma pressures in the disturbance region tend to suppress the fast earthward flows, hence the most enhanced earthward flows appear at both azimuthal sides of the disturbance region (Fig. 3.2.10(g)). The electrons and ions, injected earthward at both sides, move eastward and westward by their magnetic field drifts, respectively, in the near earth dipolarization region. Some pitch-angle scattering processes work on the electrons and cause their precipitations into the ionosphere, whereas there are no such effective pitch-angle scattering processes for the ions, whose motion becomes adiabatic and whose pitch-angle distribution becomes more trapped one. The enhanced reconnection continues at the NENL, and the source mechanism for the NPSBL aurora continues. The spatial separation between the electron precipitation by the pitch-angle scattering in the near earth dipolarization region and the precipitation from the NPSBL source region should cause the auroral "double oval" configuration during the late expansion and the recovery phases. At both azimuthal fronts of the disturbance region, the similar process from the Stage-1 to the Stage-3 occurs locally, and the expansion of the disturbance region proceeds as a result of the successive propagation of such a local stepwise evolution.

3.4. Comparison with previous models

The evolution during the Stage-1 to the Stage-2 in our schematic view in Fig. 3.2.10 is very similar to the early process in the synthesis model by *Lui* [1991a] or the model by *Erickson et al.* [2000]. Basically these models depend on some specific magnetospheric observations. Our model depends mainly on the detailed ionospheric observations, as shown in Fig. 3.2.9. We consider a consistency between those ionospheric observations and magnetospheric observations which have been studied by many authors. One of the most different points from those previous models is such that our model suggests that the rarefaction wave, launched in the near earth region, can reach the NENL location much faster than the estimations in those models. After that time, the substorm evolution should be largely

controlled by the reconnection process at the NENL. Hence, the evolution afterward is very similar to the classical NENL model [e.g. *Hones*, 1977]. One of the most important points in Fig. 3.2.10 is that the evolution of the substorm disturbance region proceeds as a successive propagation of a local stepwise evolution at both azimuthal fronts.

Sergeev et al. [1996c] stressed the importance of phenomena with a short lifetime (~1 min) in the evolution of substorm. The poleward auroral expansion is considered as a result of the successive formation of new auroral arcs ~50-100 km poleward of the previous arcs with the formation interval of 1-3 min. They considered that such a repeated appearance of the auroral arcs should be related with the repeated impulsive dissipation events (IDEs) in the plasma sheet which should be caused by the impulsive magnetic reconnection. Following their scenario, the magnetic reconnection should be active during the Stage-1 and Stage-3 in this study, and less active during the Stage-2. Such a view is consistent with our interpretation for the transition from the Stage-2 to the Stage-3. As for the successive azimuthal propagation of the substorm disturbance region, if the local first stage starts at some local time after the local first stage ends at other local time, then the unit interval of the propagation should be the duration of the local first stage, several minutes. Such a repeated evolution could correspond to the IDEs in *Sergeev et al.* [1996c].

3.5. Generality of this substorm

Since we have analyzed only one event and there were very few previous studies showing a full process of such a stepwise evolution of the auroral bulge in detail, it is very difficult to estimate whether the characteristics observed in this event are general or special ones. Undoubtedly, further event studies and statistical studies should be done in the future for that purpose.

Friedrich et al. [2001] analyzed MSP data and speculated that the poleward movement of the poleward border of 630.0 nm emission, which started 1-5 min after onset, indicates the beginning of the lobe flux reconnection at the NENL. This timing is much earlier than the start time of the Stage-3 in our event, and rather close to the start time of the Stage-2. In their figures, we can hardly see such a three stage evolution as shown in this study. The average latitude of the auroral breakup in their eight events was 67 deg, while the breakup latitude in our event was 62.7 deg, which is close to the lowest value of the latitudinal range of *Elphinstone et al.*[1995a], 65.9±3.5 deg. Hence, it could be that such a three stage evolution appears more clearly when the auroral breakup occurs at sufficiently lower latitudes.

It has been shown in previous studies that the characteristics of the auroral poleward expansion, observed from the ground, have a local time dependence, depending on the relative location to the global auroral bulge [e.g., *Akasofu*, 1964; *Fukunishi*, 1975b; *Vallance Jones et al.*, 1982]. For example, a very rapid poleward expansion of the electron auroral region without a significant poleward movement of the proton auroral region is observed on

the western side of the bulge (in the evening side) in association with a passage of the WTS. On the other hand, the poleward shift of the proton auroral region is significant on the eastern side of the bulge (in the morning side). In this event, the three stage evolution was observed at the stations at 0-1.5 hr MLT. Since there were no ground-based auroral data from other local times, and the observation by the ATV-UV was limited in an early stage of expansion phase, it is not clear in what local time range such a three stage evolution can be observed. However, considering the above-mentioned quite different characteristics of the poleward expansion in the evening and morning sides, such a three stage evolution could be observed more clearly in a certain limited local time range around the midnight, and becomes less clear at other local times.

In this event, the southward IMF condition continued through the growth phase to the expansion phase. Such an external trigger as the northward turning of the IMF did not occur at the onset time and during the expansion phase. In addition, the solar wind dynamic and static pressures were relatively high throughout the period. It should be clarified whether such IMF and solar wind conditions are relevant to the stepwise evolution. *Lyons et al.* [1997] showed the examples of the MSP data in both cases with and without the northward turning of the IMF at the onset time. The characteristics of the auroral evolution in both cases seem to be very similar to each other. It is not clear whether such a stepwise evolution as in our case can be seen in their data, because the time scale in their figures was too large to look at the evolution in an early stage of the expansion phase in detail. *Pulkkinen et al.* [1998] showed that the characteristics in the auroral bulge evolution were quite different for two substorm onsets which occurred sequentially, about 40 min apart, under the different IMF conditions. The first onset occurred under a persistently southward IMF condition, and became just a small pseudobreakup-like onset. The next one occurred after a northward turning of the IMF, and led to a major expansion of the auroral bulge. It can be said, at least, that such a significant variation of the IMF was not observed in our event in association with the stepwise evolution.

A magnetic storm developed accompanying the evolution of the substorm in this study. This storm was a moderate one [cf. *Gonzalez et al., 1994*] whose minimum Dst, -86 nT, was observed at 12 UT on June 7, 1989. The initial phase of the storm started with an SC before the start of the growth phase of the substorm, and the expansion phase of the substorm occurred during an early stage of the main phase of the storm. Hence, this substorm was a "storm-time substorm". Actually, the signatures in the injection of the energetic ions in this event are very similar to those for the "storm-time injection" in *Reeves and Henderson* [2001]. *Baumjohann et al.* [1996] showed that the substorm signatures in the magnetosphere for the "storm-time substorm" exhibit a certain difference from those for the "non-storm substorm". In the "storm-time substorm", the magnetic field dipolarization and the earthward plasma flow in the near-earth tail after onset are much more pronounced than in the case of the

"non-storm substorm". The decrease of the lobe magnetic pressure during the expansion phase is observed only in the "storm-time substorm". They speculated that the reconnection of the open magnetic field lines at the NENL should occur only in the "storm-time substorm". Based on their speculation and our interpretation in Fig. 3.2.10, such a three stage evolution as in this event could be observed only in the "storm-time substorm".

Baker et al. [1993] analyzed one special event in detail using a great amount of data obtained both in the magnetosphere and ionosphere. The expansion phase onset of the substorm occurred around the maximum period of a storm (minimum Dst = -79 nT) during a very disturbed period (AE = 860 nT) after the recovery phase of a previous substorm. On the other hand, the substorm in our study was the first one which occurred after a prolonged quiescent period. Despite such a difference in the magnetospheric and ionospheric conditions before the onset, the auroral bulge evolution shown in *Baker et al*. [1993] was quite similar to our event as follows. Looking at their Plate 2, the initial auroral brightening occurred at lower latitudes separated from a poleward-most activity which clearly appeared before the onset. The initial poleward expansion was very rapid and reached the poleward-most activity at least 3 min after the onset, and the expansion proceeded predominantly in the azimuthal direction afterward. A clear further poleward expansion appeared about 16 min after the onset. Hence, such a stepwise evolution of the auroral bulge might not significantly depend on the disturbance level in the magnetosphere and ionosphere before the onset.

4. Summary and Conclusions

We have analyzed in detail the auroral bulge evolution during the expansion phase of an isolated substorm, which was observed by the UV auroral imager aboard AKEBONO and the ground-based optical instruments at SYO and ASK. A detailed observation summary is described in the section 3.1. Several important points of this study are summarized briefly as follows:

1. We presented a clear example which shows a systematic stepwise evolution of the auroral bulge and SCW system during the expansion phase, and analyzed the characteristics of the evolution during each stage in detail.
2. Detailed comparison between the satellite global auroral data and the ground-based optical observations showed that the global evolution should proceed as a successive propagation of the local three-stage evolution.
3. The NPSBL aurora is considered to be a key auroral activity in this study. It should play a very important role in the auroral bulge evolution.

Based on these observations, we discussed the evolution in the magnetosphere during the expansion phase. This event was a very ideal and very fortuitous one. Further event studies and statistical studies are necessary for clarifying whether the several important points which

can be seen in this event are generally observed in other substorms or this event is a very special one. For such studies, simultaneous observations both of the global auroral evolution and the local detailed auroral evolution should be essentially important.